A study of long-term trends in mineral dust aerosol distributions in Asia using a general circulation model

Makiko Mukai and Teruyuki Nakajima
Center for Climate System Research, University of Tokyo, Tokyo, Japan

Toshihiko Takemura
Research Institute for Applied Mechanics, Kyushu University, Fukuoka, Japan

Received 22 October 2003; revised 10 May 2004; accepted 10 June 2004; published 9 October 2004.

[1] Dust events have been observed in Japan with high frequency since 2000. On the other hand, the frequency of dust storms is said to have decreased in the desert regions of China since about the middle of the 1970s. This study simulates dust storms and transportation of mineral dust aerosols in the east Asia region from 1981 to 2001 using an aerosol transport model, Spectral Radiation-Transport Model for Aerosol Species (SPRINTARS), implemented in the Center for Climate System Research/National Institute for Environmental Studies atmospheric global circulation model, in order to investigate the main factors that control a dust event and its long-term variation. The model was forced to simulate a real atmospheric condition by a nudging technique using European Centre for Medium-Range Weather Forecasts reanalysis data on wind velocities, temperature, specific humidity, soil wetness, and snow depth. From a comparison between the long-term change in the dust emission and model parameters, it is found that the wind speed near the surface level had a significant influence on the dust emission, and snow is also an important factor in the early spring dust emission. The simulated results suggested that dust emissions from northeast China have a great impact on dust mass concentration in downwind regions, such as the cities of northeastern China, Korea, and Japan. When the frequency of dust events was high in Japan, a low-pressure system tended to develop over the northeast China region that caused strong winds. From 2000 to 2001 the simulated dust emission flux decreased in the Taklimakan desert and the northwestern part of China, while it increased in the Gobi desert and the northeastern part of China. Consequently, dust particles seem to be transported more from the latter region by prevailing westerlies in the springtime to downwind areas as actually observed. In spite of the similarity, however, there is still a large disagreement between observed and simulated dust frequencies and concentrations. A more realistic land surface and uplift mechanism of dust particles should be modeled to improve the model simulation. Desertification of the northeastern China region may be another reason for this disagreement. *INDEX TERMS:* 0305 Atmospheric Composition and Structure: Aerosols and particles (0345, 4801); 0399 Atmospheric Composition and Structure: General or miscellaneous; 1630 Global Change: Impact phenomena; 1699 Global Change: General or miscellaneous; 3665 Mineralogy and Petrology: Mineral occurrences and deposits; *KEYWORDS:* dust, Asia, aerosol

Citation: Mukai, M., T. Nakajima, and T. Takemura (2004), A study of long-term trends in mineral dust aerosol distributions in Asia using a general circulation model, *J. Geophys. Res.*, *109*, D19204, doi:10.1029/2003JD004270.

1. Introduction

[2] A characteristic atmospheric event in the spring season over the east Asian region is an atmospheric dust event, called 'Kosa' in Japanese, a phenomenon in which sand and soil particles are raised and transported by storms to make the atmosphere turbid and yellow in color. Major sources of the Asian dust are located in arid and semiarid regions such as Gobi, other deserts, and the Loess Plateau. Dry surface conditions and a strong wind are necessary for causing these dust storms. In this regard, dust storms are a result of interaction between the weather conditions and the land surface conditions [*Yang*, 2002]. Dusts have various impacts on the environment and human society. Mineral dusts affects the radiation balance through their scattering and absorbing solar and thermal radiation as well as affecting the atmospheric composition through their chemical reaction in the air. It is also recognized that small soil particles in the air are harmful to the human respiratory

0148-0227/04/2003JD004270$09.00

system, and furthermore, strong dust storms can damage people, livestock and cultivated fields. The cleaning cost in urban areas is also significant.

[3] Dust storms in China have shown a decreasing tendency from the mid 1970s [*Qian et al.*, 2002]. On the other hand, in Korea, the occurrence of dust appears to be more frequent during the last decade [*Chun et al.*, 2001]. In Japan, days with Asian dust events have rapidly increased since 2000 as observed at weather observatories of the Japan Meteorological Agency. It is difficult, however, to understand what factors are controlling the long-term trends and regional differences from only an analysis of the meteorological data as done by previous studies. This study, therefore, tries to investigate the controlling factors of the dust event through a long-term simulation of the events from January 1981 to October 2001 using an aerosol transport-radiation model implemented in an atmospheric general circulation model (AGCM). The simulated frequency and magnitude of Asian dust are compared with observed data in order to find the main factors that control the trend.

2. Model Description

[4] In this study, we used a three-dimensional aerosol chemical transport model called the Spectral Radiation-Transport Model for Aerosol Species (SPRINTARS) developed at the Center for Climate System Research (CCSR), the University of Tokyo [*Takemura et al.*, 2000, 2002a, 2002b]. The model treats carbonaceous (organic and black carbons), sulfate, soil dust, and sea salt aerosols. The aerosol transport process includes emission, advection, diffusion, sulfur chemistry, wet deposition, dry deposition, and gravitational settling. It is driven by an atmospheric general circulation model (AGCM) of CCSR and the National Institute for Environmental Studies (NIES), Japan [*Numaguti et al.*, 1995]. The horizontal resolution of triangular truncation is set at T42 (approximately 2.8° by 2.8° in latitude and longitude) and the vertical resolution at 11 layers (sigma level based on the surface pressure at 0.995, 0.980, 0.950, 0.900, 0.815, 0.679, 0.513, 0.348, 0.203, 0.092 and 0.021). The model is forced to simulate real atmospheric conditions by a nudging technique using European Centre for Medium-Range Weather Forecasts (ECMWF) reanalysis data on wind velocities, temperature, specific humidity, soil wetness and snow depth.

[5] The dust particle radius is divided into 10 size bins from 0.1 to 10 μm. Emission locations are limited to desert, grassland, and xeromorphic shrubland defined by *Matthews* [1983]. Figure 1 is a map of the potential emission areas in this model. It includes major deserts such as the Sahara, deserts in the Middle East, deserts in Asia and so on. The potential emission areas are fixed and desertification is not considered. The dust emission process is modeled by locations, near surface wind speed above a threshold, and soil wetness and snow depth below their thresholds. Under these conditions, the emission mass flux of the soil dust is calculated according to the semiempirical relation as follows [*Gillette*, 1978]:

$$F = C(|\mathbf{v}_{10}| - v_t)|\mathbf{v}_{10}|^2 \quad \text{for} |\mathbf{v}_{10}| \geq v_t$$
$$F = 0 \quad \text{for} |\mathbf{v}_{10}| \leq v_t, \tag{1}$$

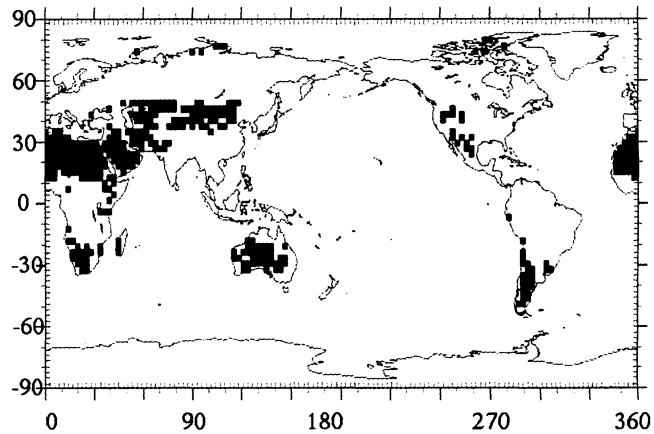

Figure 1. A map of the potential emission areas in this model.

where $\mathbf{v}_{10}$ is the wind velocity at 10 m height in ms^{-1}, v_t is the threshold velocity set at 6.5 ms^{-1} according to *Kalma* [1988], and C is an emission coefficient depending on the soil wetness as

$$C = 1.3 \times 10^{-9} \times \frac{S_t - S}{S_t} \quad \text{for } 0 \leq S \leq S_t,$$
$$C = 0 \quad \text{for } S \geq S_t, \tag{2}$$
$$C = 0 \quad \text{for } D \geq D_t,$$

where S is the soil wetness, S_t is the threshold soil wetness, D is the snow depth and D_t is the threshold snow depth. The emission mass flux of soil dust is assumed to be zero when the snow depth is larger than the threshold. In this study, the threshold soil wetness in the Asian region is set at 0.22 $\mathrm{m}^3\ \mathrm{m}^{-3}$, and the threshold snow depth is set at 0.005 m. These thresholds are determined by fitting the modeled aerosol optical thickness to the AVHRR-retrieved optical thickness over the ocean near dust regions. Vertical uplift levels of aerosols at emission are mainly determined using the potential temperature of each layer and the surface temperature in this model. Dust aerosols are emitted with a constant mixing ratio from the lowest model layer to the layer whose potential temperature is lower than the surface temperature:

$$q_a = q_{a0} + \frac{Fg\Delta t}{p_0 - p_{\theta<T_S}}, \tag{3}$$

where q_{a0} is the aerosol mixing ratio before the time step, g is the gravitational constant, Δt is the model time step, p_0 is the surface pressure, and $p_{\theta<T_S}$ is the pressure at the highest layer whose potential temperature is lower than the surface temperature. The vertical diffusion flux is calculated as follows:

$$F_D = -\rho_{\mathrm{air}} K \frac{\partial q_a}{\partial z}, \tag{4}$$

where F_D is the vertical diffusion flux, ρ_{air} is the air density, and K is the diffusion coefficient. This model also takes into consideration a simple shallow convection using the saturated specific humidity q^* and the humid static energy

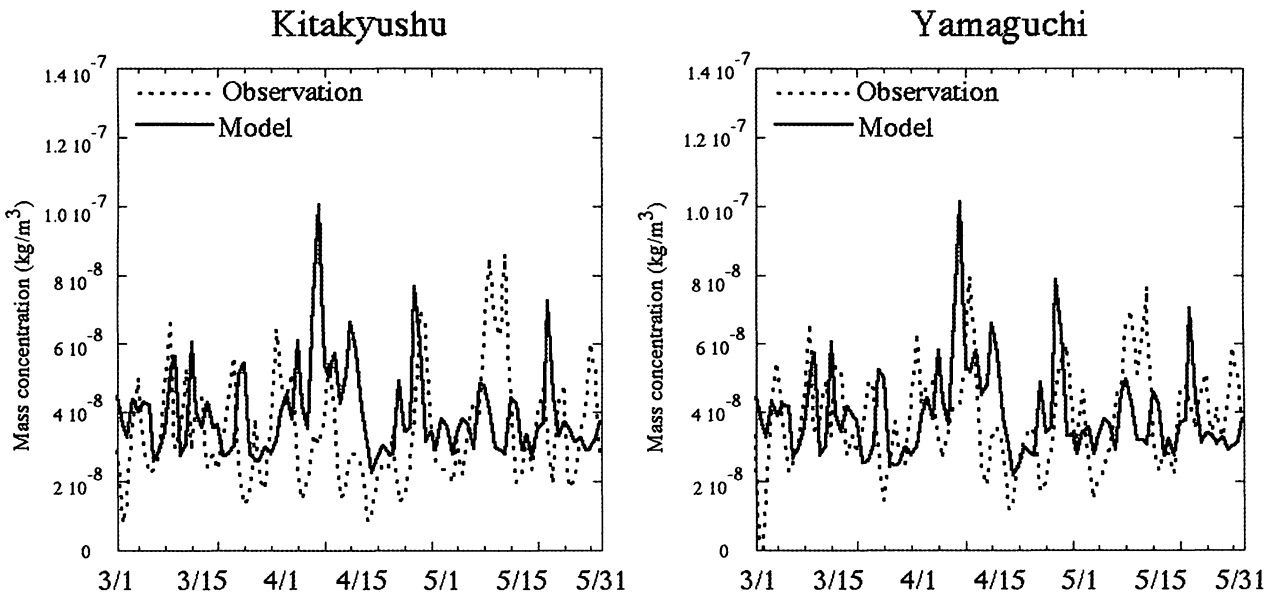

Figure 2. Comparison between simulated and observed aerosol mass concentrations (kg/m^3). Dotted lines show observed concentrations of suspended particulate matter, provided by the National Institute for Environmental Studies, and solid lines show modeled aerosol mass concentration near the surface as the sum of mass concentrations for the carbonaceous, dust, sulfate, and sea salt aerosols at Kitakyushu City and Yamaguchi City, in Japan, in 1990 from March to May.

h. If the following formula is satisfied, aerosol mixing ratios of the kth and the $k+1$th layers are given as same:

$$h_k > h^*_{k+1}$$
$$q^*_w(T') < q_{w,k} \quad \left(T' = \frac{h_k - gz_{k+1} - Lq_{w,k}}{C_p}\right), \tag{5}$$

where k is the model layer number, h^* is the saturated humid static energy, q_w is the specific humidity, L is the latent heat of evaporation for water, and C_p is the atmospheric specific heat at constant pressure.

[6] We first compared aerosol distributions with and without dust emission in the Asian regions including the Gobi desert and the Taklimakan desert to study the contribution of dust emission from other deserts. Simulated spring mean aerosol mass concentrations at near the surface level in cities of east Asia decreased by more than 90% by removing the Asian dust emission. Therefore a dust aerosol emitted from Asia regions has a great influence on the dust concentration near the surface in east Asian cities, and the influence from other deserts is found to be weak in spring, especially in the east Asian region in our discussion. Also, it should be remembered that an observed dust event day is determined based on the visibility, so that the total aerosol concentration including dust emission from all the deserts in the world will be a better quantity for comparison with observed dust event days.

3. Results and Discussion

3.1. Comparison Between Simulated and Observed Results

[7] We simulated the Asian dust events from January 1981 to October 2001 using the model. We did not change the land surface types and conditions, other than the soil wetness and snow depth, during the simulation period in order to study the effect of the meteorological parameters in the dust events without including desertification and land use change impacts which are very uncertain and difficult to model. Figure 2 compares the simulated daily aerosol mass concentration with the corresponding observed data in March–May 1990, the main dust storm season, obtained at Kitakyushu City (33°53′N, 130°52′E) and Yamaguchi City (34°10′N, 131°28′E). The modeled values were calculated as the total aerosol mass of the simulated dust, carbonaceous, sulfate and sea salt aerosol mass concentrations during the same period. The observed values are the mass concentration of suspended particulate matter measured as daily ambient air quality data from the Environmental Information Center, NIES (National Institute for Environmental Studies). The figure shows that the model well reproduced the magnitude and peak features of the mass concentration similar to the observed ones, although accurate magnitude and timing of each peak are difficult to simulate.

[8] Figures 3a–3c show a time series of simulated total aerosol mass concentrations near the surface averaged from March to May and the observed number of days with a dust event at Nagasaki (32°45′N, 129°52′E), Seoul (37°32′N, 126°58′E), and Beijing (39°55′N, 116°26′E). The Japan Meteorological Agency (JMA) defines the day of observing dust events as a *Kosa*-day, a day when the visibility is less than 10 km. We quote the observed number of days with dust events at Seoul from 1981 to 1999 from *Chun et al.* [2001] and Beijing (39°55′N, 116°26′E) from 1981 to 1999 from *Qian and Zhu* [2001]. We also display a time series of the March–May mean observed suspended particulate matter concentrations from 1981 to 2001 at Nagasaki. Note that

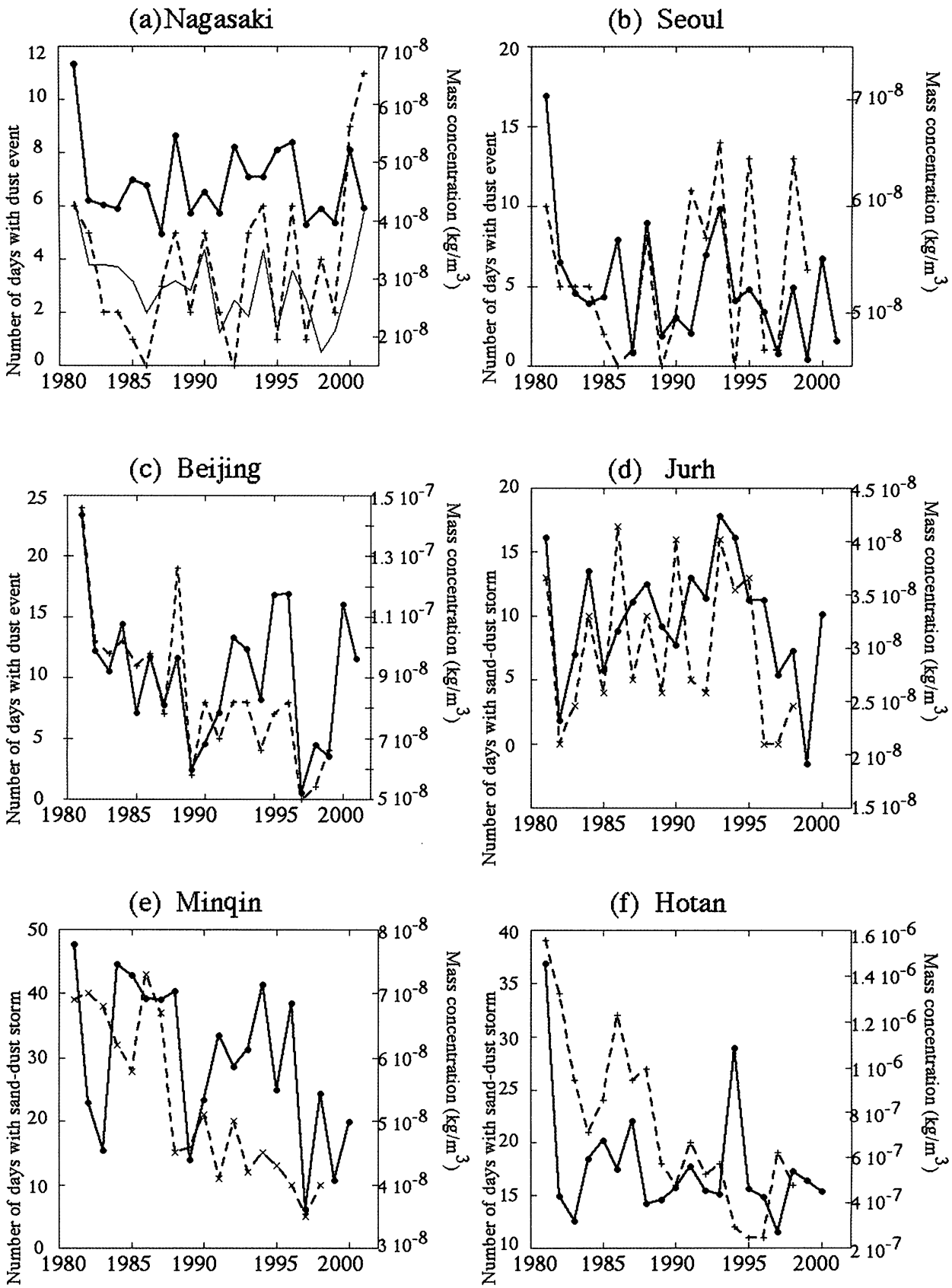
(a)Nagasaki
(b) Seoul
(c) Beijing
(d) Jurh
(e) Minqin
(f) Hotan
Number of days with dust event
Number of days with sand-dust storm
Mass concentration (kg/m3)
1980
1985
1990
1995
2000

Figure 3

these observed data do not include the mass concentration of particles larger than 5 μm in radius, so that the observed mass concentration is smaller than the modeled aerosol mass concentration. The observed number of days with a dust event decreased from 1981 to 1986 at three locations. After that, the frequency of dust events in Beijing continued decreasing, while the frequency in Seoul was complicated but was relatively high in 1990s, and the frequency in Nagasaki also had large fluctuations and increased rapidly after 2000.The figure also shows a short-term fluctuation with a period of 4 to 6 years, as also reported by *Yoshino* [2001]. In Beijing, the trend of the model is consistent with that of observation and the correlation coefficient between observation and the model is 0.74. Here the correlation coefficient is calculated as

$$\text{correlation coefficient} = \frac{\frac{1}{N}\sum_{i=1}^{N}(x_i - x_{\text{mean}})(y_i - y_{\text{mean}})}{\sigma_x \sigma_y}, \quad (6)$$

where $\{x_i\}$ are model values, $\{y_i\}$ are observed data, x_{mean} and y_{mean} are mean values for data sets $\{x_i\}$ and $\{y_i\}$ respectively, σ_x and σ_y are the corresponding standard deviations, and N is the number of data. The main features and timing of the peaks in the time series of the simulated result in Seoul are almost similar to that of the observed number of days, although there are a few years showing a discrepancy between model and observation that makes the correlation of long-term trends between modeled and observed values worse as 0.40 than that of the Beijing case. Simulated results in Nagasaki are similar to the observed trends with peaks in 1981, 1988, and 1996, though peaks in 1992 and 1995 have no corresponding peaks in the observed time series and the large *Kosa*-day numbers in 2000 and 2001 are not very obvious. The correlation coefficient of the model and the observed numbers of *Kosa*-days in Nagasaki is 0.40. The model needs, therefore, a more accurate long-range transportation and emission source distribution of mineral dust aerosols to simulate the detailed distribution of dust concentrations over Korea and Japan. It may also need to take into account the effect of local air pollution, which may lead to a misjudgment of dust events by meteorological agencies. In this regard, it should be noted that modeled global distributions of mineral dust aerosol optical thickness and single scattering albedo have been compared with data from the AERONET network of sky-Sun photometers and were found to show reasonable agreement between modeled and observed values [*Takemura et al.*, 2002a, 2002b; *Kinne et al.*, 2003; *Nakajima et al.*, 2003; *Takemura et al.*, 2003]. In order to investigate the features of the dust storm variation inside arid areas, we compare in Figures 3d–3f time series of the annual mean modeled total aerosol mass concentrations and the number of days of observed dust storms at Hotan (37°06′N, 79°54′E) in the southern part of the Taklimakan desert, Minqin (38°36′N, 103°06′E) on the Hexie Corridor and Jurh (42°24′N, 112°54′E) in Inner Mongolia from 1981 to 1998 as adopted from *Yoshino* [2001]. Observed dust day numbers in inland China show a clear decreasing trend, while the trend in Jurh is different from that in other locations as also pointed out by *Yoshino* [2001]. The correlation coefficient in Hotan is 0.35. Model results show an extreme decrease in 1982 and too strong a peak in 1994. The correlation coefficient calculated without these two years is 0.66. In Minqin, the correlation coefficient is 0.32. However, if the excessive decrease from 1982 to 1983 is excluded from calculating the correlation coefficient, it becomes 0.60. In Jurh, the time series of simulated results almost agree with that of observation, and the correlations coefficient is 0.58.

3.2. Relation Between Modeled Dust Emission and Aerosol Mass Concentration

[9] Figure 4 shows the simulated distribution of the spring mean dust emission flux averaged from 1981 to 2001. There are a few strong emission areas, the first of which is the Taklilmakan desert and western China deserts from 75°E to 95°E and from 35°N to 45°N. The second is the Central Gobi desert from 95°E to 110°E and the northeast China region from 110°E to 120°E near Beijing. Also shown is the dust emission from the Great Indian desert around 70°E and from 25°N to 30°N. We have explained in section 2 that dust emitted from Asian regions has a great influence on the dust concentration near the surface in east Asian cities. Therefore we investigate the relation between the dust emission from Asian deserts from 75°E to 120°E and 35°N to 50°N and the aerosol mass concentration in east Asian cities in this section.

[10] Figure 5 displays correlation coefficients of spring mean modeled total aerosol mass concentrations in Beijing, Seoul, and Nagasaki with spring mean dust emission fluxes in Hotan, Minqin, and Jurh. The most influential region for the long-term trend of the total aerosol mass concentration in the three cities is Jurh, located in the Inner Mongolia area. The time series of dust emission in Jurh is in good agreement with that of the total aerosol mass concentration near the surface in these downwind cities. It is found that the modeled mass concentrations in Beijing, Seoul and Nagasaki are strongly influenced by dust emission in the northeast China region as is the emission in Jurh, because this region is near these cities. The correlation between the mass concentration in Beijing and the dust emission in Minqin shows a high value next to that in Jurh. Dust

Figure 3. Time series of aerosol mass concentration (kg/m^3) and observed days. (a–c) Modeled total aerosol mass concentrations near the surface level averaged from March to May from 1981 to 2001 in Nagasaki, Seoul, and Beijing (solid lines), and the observed number of days with dust events from 1981 to 2001 in Nagasaki and from 1981 to 1999 in Seoul and Beijing (dashed lines). The thin solid line in Nagasaki indicates observed concentrations of suspended particulate matter, provided by the National Institute for Environmental Studies, from 1981 to 2001. (d–f) Annual mean modeled total aerosol mass concentrations near the surface level from 1981 to 2000. Dashed lines show observed numbers of days with sand-dust storms from 1981 to 1999 at Hotan in the southern part of the Taklimakan Desert, Minqin, on the Hexie Corridor and Jurh in Inner Mongolia.

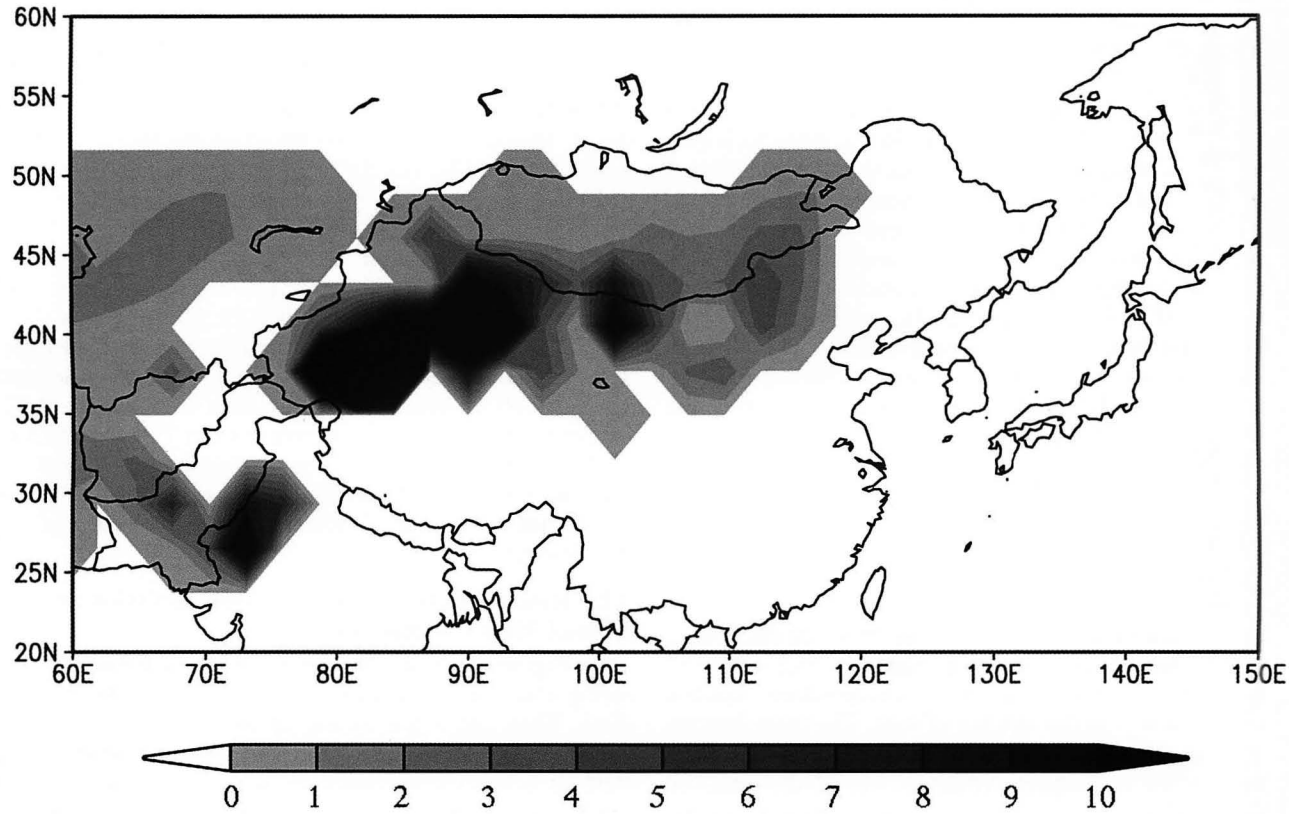

Figure 4. Spring mean simulated dust emission flux ($\mu g/m^2/s$) averaged from 1981 to 2001.

emission in Hotan is influential for the mass concentration in Seoul and Nagasaki next to that in Jurh.

[11] In the model simulation, the long-term trend in the aerosol mass concentration is almost uniquely controlled by that of the simulated dust emission flux. Especially, mass concentrations in the cities of China, Korea and Japan are simulated to be strongly affected by dust emission in northeast China. Therefore one of the reasons that the large increase after 2000 is not as obvious in the model simulation is that our model failed to simulate the large increase in the dust emission that originated from the northeastern part of China. It will be necessary to study the impact of the recent desertification trend in this region, which is not included in the present simulation. The trend in the aerosol mass concentration in Nagasaki interrelates with that of the dust emission flux in Hotan. The uncertainty of the simulated dust emission may be one of the causes of uncertainty in the modeled aerosol mass concentration in Nagasaki. Hence it is important for study of the long-term trend of Asian dust events to investigate dust emission in these source regions.

[12] A comparison between simulated results and observed data in the previous subsection confirms that the model calculation driven by objective analysis meteorological data can partly reproduce the main features of the temporal trend and the spatial distribution of dust aerosols. In order to understand the mechanism of the variation in dust events, we investigate in this subsection the dependence of the simulated results on various factors in the model processes. We first calculate in Figure 6 the anomaly of the total aerosol mass concentration near the surface level and the dust emission flux averaged for five subperiods, 1981–1984, 1985–1989, 1990–1994, 1995–1999, and 2000–2001, relative to the mean value of the whole period. The figure shows that temporal and spatial variations in mass concentration and dust emission

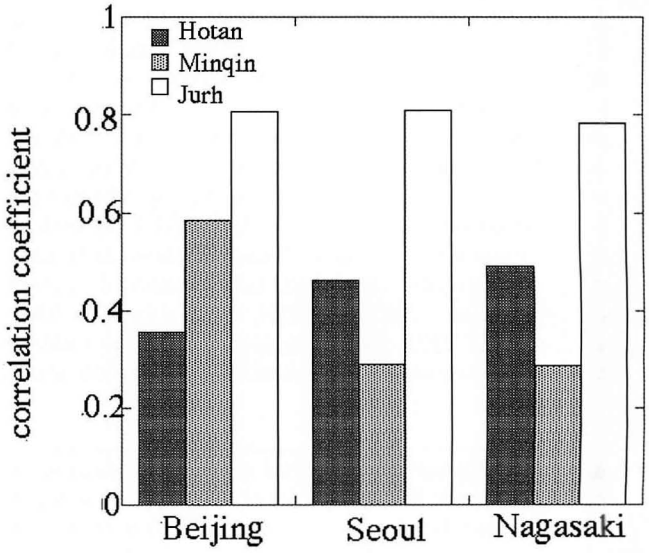

Figure 5. Correlation coefficient of the time series of spring mean modeled total aerosol mass concentration near the surface level in Beijign, Seoul, and Nagasaki and that of spring mean dust emission flux in Hotan, Minqin, and Jurh.

anomalies resemble each other, which is easily understood because the aerosol mass concentration in spring is mainly affected by dust emissions within the area that is several hundred kilometers wide around the location due to their short lifetime. Another clear observation in the figure is that the dust emission flux in March increased during these periods, while the May emission decreased. Table 1 summarizes the monthly mean simulated dust emission flux in the Taklimakan desert region (37°–43°N, 75°–92°E) and the Gobi desert region (37°–48°N, 95°–120°E) from March to May averaged for the five subperiods from 1981 to 2001. In order to discuss this point in more detail, we compare Figures 6a–6c and Table 1. The dust emission flux increased in March for the whole period in the Gobi desert and northeast China region, whereas the Taklimakan desert region had some oscillatory variations depending on the period, i.e., a large emission in 1995–1999, but a small emission in 2000–2001. The April dust emission anomaly was more complicatedly varied other than a strong increase in 2000–2001 over the Gobi desert. In May there was a general decreasing trend in emission, though each part of the region underwent a complicated variation depending on the period. In summary it is notable that the dust emission in the Gobi desert and northeast China increased in March and decreased in May. This fact consequently explains that these emission areas near the cities of northeast China, Korea, and Japan have the potential to cause a large increase in the dust mass concentration and the dust days in these east Asian areas with prevailing westerlies common in springtime, especially for the large Asian dust events in 2000–2001. In this model, however, dust emitted from the Taklimakan desert also impacted on the mass concentration near the surface over Japan as shown in the previous section, so that the recent decreasing tendency of dust emission from the Taklimakan desert may be one of the reasons why the model failed to simulate the large increase in the dust mass concentration after 2000.

3.3. Meteorological Factors Controlling Asian Dust Events

[13] The comparison between simulated results and observed data in the previous subsection confirms that the model calculation driven by objective analysis meteorological data can partly reproduce the main features of the temporal trends and the spatial distribution of dust aerosols. In order to understand the cause of variations in dust events in the model, we investigate in this subsection the dependence of simulated results on various factors in the model processes. To investigate the main factors that control the long-term variation in the modeled dust emission, we plot in Figure 7 the time series of March, April and May mean dust emission flux, snow depth, soil wetness, and wind speed in the Gobi desert (37°–48°N, 95°–120°E) and the Taklimakan desert (37°–43°N, 75°–92°E) as derived from the model. The dust emission in the Taklimakan desert is much greater than that in the Gobi desert, because the wind speed is greater, the soil is drier, and the snow is less in the Taklimakan. The main control factor of the trend in dust emission is the wind speed near the surface, as understood by the parameterization of the emission proportional to the 3rd power of the wind speed in equation (1). It is assumed that in the mid-1990s a decrease in snow produced an increase in the dust emissions in both deserts, whereas in the 1980s, an increase in soil wetness caused a decrease in the dust emission. It is thought that the influence of these factors changes their contribution depending on the area and month. In the Gobi desert, the time series of wind speed at 10 m is similar to that of dust emissions with some peaks in March and April. Snow restrains the dust emission in March. The impact of the snow depth decreases with melting snow. Dust emissions in March and April increased from 2000 to 2001, but the dust emissions in May decreased, so that the spring mean dust emissions did not show a rapid increase in this period. In the Taklimakan desert, the correlation of wind speed with dust emission is high through out the spring. The change in soil wetness is not so much reflected in that of the dust emissions. The increased dust emission in early spring, as indicated in Figure 6, was caused by a decrease in snow, specially the small snow amount in 2001. An increasing tendency in soil wetness causes a decrease in the dust emission in May in the Gobi desert. When the model overestimates the dust emission, such as the too strong peak in 1994 in the Taklimakan desert, not only is the surface wind simulated to be too strong but also the soil wetness is too small. Hence the treatment of soil wetness is important for simulating dust emissions.

3.4. Seasonal Variation in Asian Dust Events and Its Controlling Factors

[14] Global distributions of UV-absorbing aerosols are obtained from the Total Ozone Mapping Spectrometer (TOMS). Major sources of UV-absorbing aerosols are biomass burning and desert dust aerosols. Figure 8 compares the monthly mean distribution of the TOMS aerosol index and distributions of dust optical thickness and carbonaceous aerosol optical thickness from the model in 2000. In the satellite data, dust aerosols started to appear in the desert region from March until May, decreased after the spring season, and then disappeared in the winter. In the model results, the dust optical thickness gradually increased since March and was maintained until July. In both the observation and model results, large values appear in the latitudinal zone of 75°–90°E corresponding to main dust aerosol plumes emitted from the Taklimakan desert. Also from spring to summer, high values around the left corner of the figures seem to be caused by biomass burning aerosol and dust emission from deserts located to the west of China, even from the Middle East. Aerosols around 100°E to 120°E from March to May were mainly emitted from the Gobi desert. However, the optical thickness value is less than that around the Taklimakan desert. The satellite does not detect aerosols from October to February over the east Asia region, but the model generates weak aerosols over the Taklimakan desert region.

Figure 6. Time series of the distributions of the anomaly in dust emission flux (left panels, $\mu g/m^2/s$) and total aerosol mass concentration near the surface level (right panels, $\mu g/m^3$) averaged for terms 1981–1984, 1985–1989, 1990–1994, 1995–1999, and 2000–2001 for each month: (a) March mean, (b) April mean, and (c) May mean.

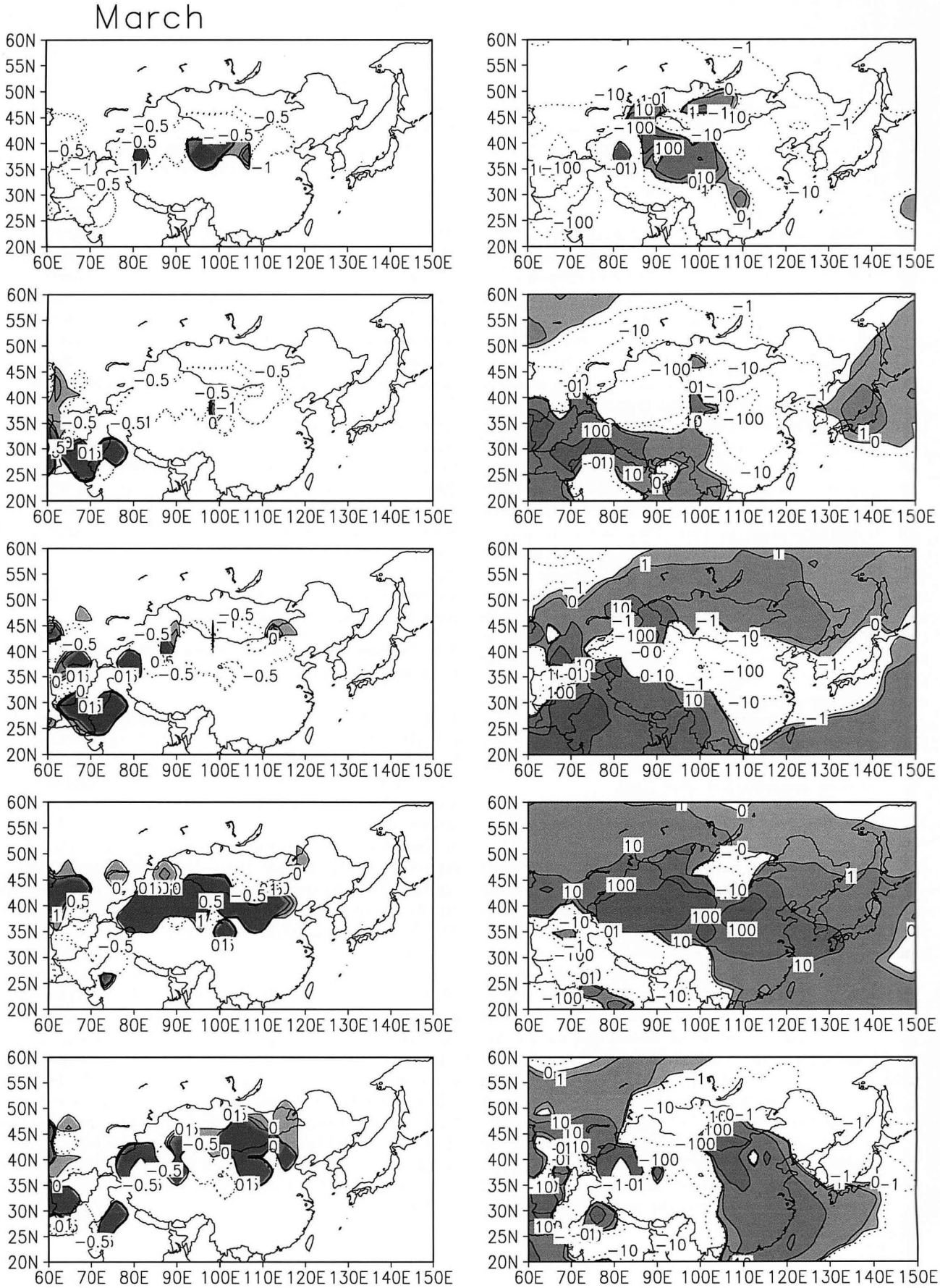
March
60N
55N
50N
45N
40N
35N
30N
25N
20N
60E 70E 80E 90E 100E 110E 120E 130E 140E 150E

Figure 6

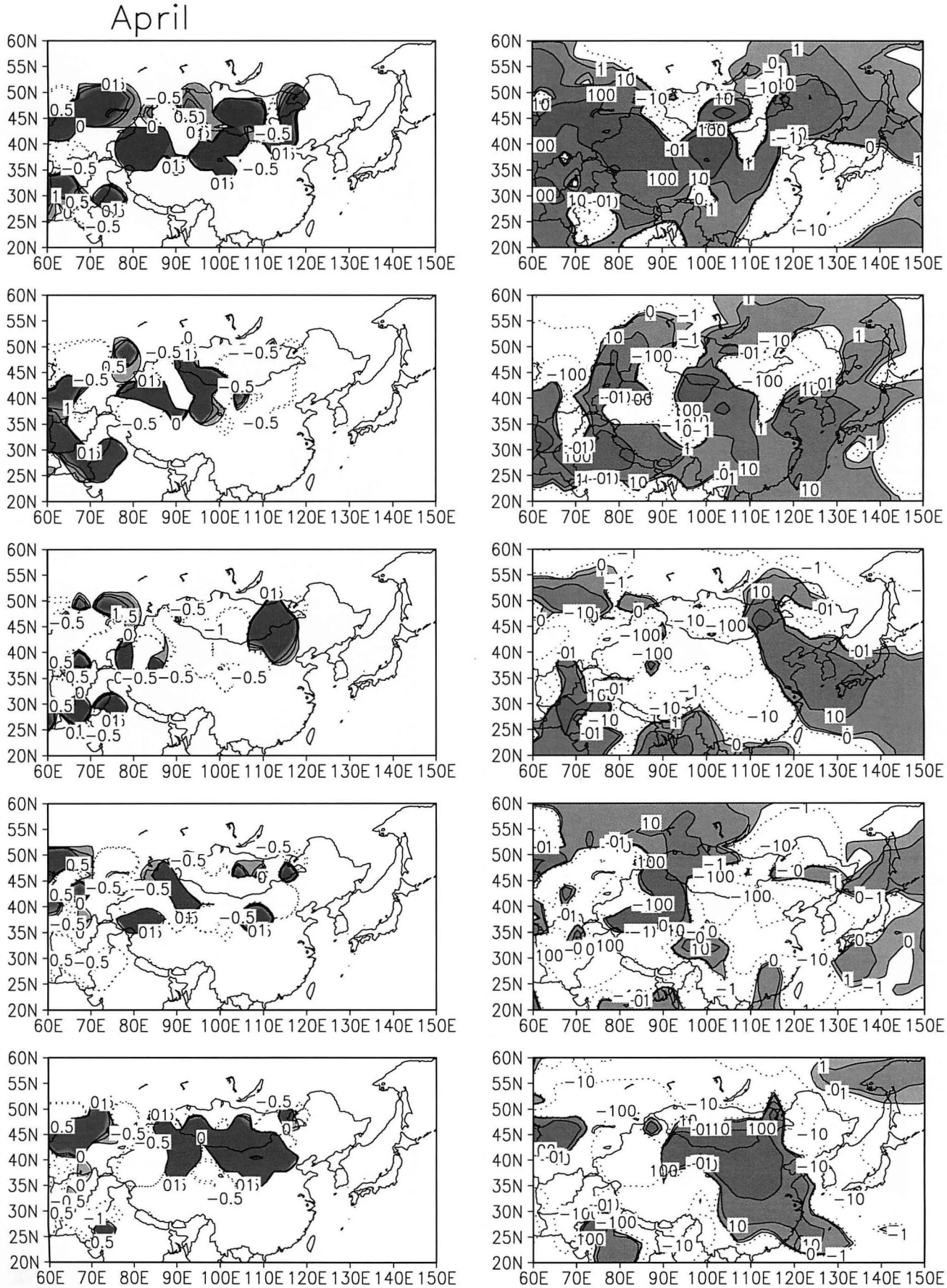

Figure 6. (continued)

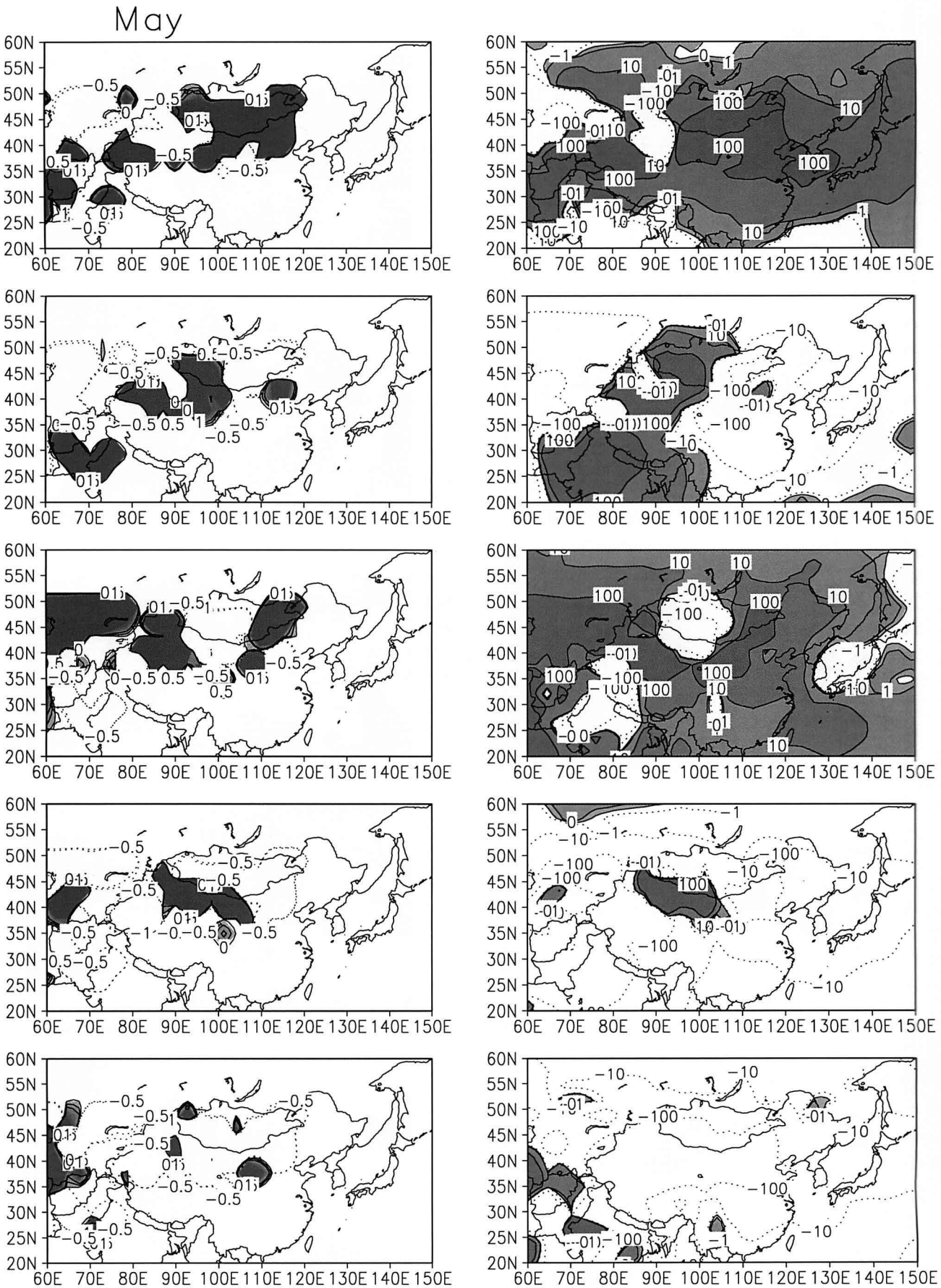

Figure 6. (continued)

Table 1. Simulated Dust Emission Flux Averaged for Periods 1981–1984, 1985–1989, 1990–1994, 1995–1999, and 2000–2001 in March, April, and May in the Taklimakan Desert and the Gobi Desert[a]

	Taklimakan			Gobi		
	March	April	May	March	April	May
1981–1984	31.3	32.0	23.6	1.85	7.45	8.66
1985–1989	28.7	28.6	21.1	1.48	5.45	5.38
1990–1994	29.9	26.3	22.1	1.62	6.54	5.88
1995–1999	33.1	32.6	21.8	3.57	5.54	5.91
2000–2001	17.7	22.9	13.6	3.85	11.6	3.46

[a]Flux in $\mu g/m^2/s$.

[15] To investigate the conditions determining such seasonal variations in the dust emission in this model, we plot in Figure 9 the monthly mean dust emission flux, wind speed near the surface, soil wetness, and snow depth in the Gobi desert and the Taklimakan desert. Spring has a strong dust emission in both deserts. The air and ground conditions in the spring are suitable for dust emission because of a strong surface wind, less snow and dry land conditions. In the summer, on the other hand, winds become weaker and the land becomes moist, so that dust emission becomes weak. In the autumn and winter, surface winds become stronger but moist land and snow cover suppress the dust emission. This general scenario of the seasonal variation in the dust emission is modified for each region of significant dust emission. In the Gobi desert, most dust emissions happen in April–May, while the Taklimakan desert also emits dust particles in winter because of a lower snow amount and stronger surface wind speed as compared to the Gobi desert conditions. The surface wind speed is found to have the largest impact on dust emission, but soil wetness and snow cover are also important depending on the season of the year. The effects of soil wetness and snow on dust emission are variable depending on each of the threshold values for dust emission, hence the surface conditions. In this regard, our model treatment of the ground conditions may be too simple to simulate such delicate long-term and seasonal variations complicatedly controlled by surface conditions.

4. Discussion

[16] In the previous section, a strong correlation between dust emission and wind speed near the surface level was shown. This result agrees with previous reports that the frequency of dust storms closely correlates with the surface wind velocity. It is said that strong winds in the Chinese and Mongolian deserts are associated with cold air outbreaks, which result from the occurrence of frontal systems and low pressure [*Sun et al.*, 2000]. We investigated the relationship between mean dust conditions in high-dust-frequency years and those in low-frequency years. In the period from 1981 to 2001, the years with high numbers of observed dust events in April in Japan are 1988, 1990, 1993, 2000 and 2001. On the other hand, the low-number years are 1982, 1984, 1986, 1987 and 1991.

[17] When dust events frequently occurred, the Pacific high-pressure system tended to be weak and a low pressure was located in northeast China that caused more dust events in the Gobi desert and northeast China region, as shown in Figure 10 which displays mean sea level pressure distributions in April in high- and low-frequency years. On the other hand, the low-frequency years correspond to the years of prevailing Pacific high and weak low pressures in northeast China. Figure 11 shows the difference between the high-frequency year wind speed and the low-frequency year wind speed at 700 hPa. In April, the west-northwest wind was dominant every year in this region. Corresponding to this pressure anomaly, the high-frequency years tended to develop a cyclonic wind field over the Japan Sea and hence a westerly wind anomaly from northern China toward western Japan that efficiently brought dust particles to Korea and Japan. Figure 12 shows the difference between the surface temperature in March of the high-frequency years and that in the low-frequency years. When the frequency of dust events was high in April, the surface temperature in March was higher than the low-frequency year mean temperature in the northern part of China and Mongolia causing early snow melting in these regions. In order to see this situation in our simulated results, we show in Figure 13 the difference between the means of the simulated dust mass concentration in high- and low-dust-frequency years. When dust events were frequently observed, the simulated mass concentration was higher in eastern and southern China and the adjacent ocean region which covers the major cities in China, Korea and Japan. This shows that these simulated results do not contradict the observed number of days with dust events in Japan. Figure 14 shows the difference in dust emission fluxes between high- and low-frequency years. It is found from Figures 13 and 14 that the increased dust concentration in the major cities of east Asia observed in the high-frequency years was mainly caused by the dust emission from the Gobi desert and northeast China, while the dust emission from the Taklimakan desert was small.

5. Conclusions

[18] According to our simulation results, the most important factor in the long-term variation in dust emission is the wind speed near the surface level in the period from March to May, consistent with the past analyses of meteorological data. Early spring snow is also an influential factor in dust emission, suggesting that the recent decrease in snow in spring tends to trigger more dust events in the Gobi and northeastern China regions. Soil wetness impacts on the seasonal variation in dust emission through out the entire year. A comparison between high- and low-frequency years of dust events shows that when the frequency of dust events was high, a low pressure frequently developed over northeast China and caused strong winds. Furthermore, the high pressure over the Pacific Ocean tended to be weak, and westerly winds from northern China toward western Japan became stronger in the high-dust-frequency years. These meteorological conditions produced a good condition for dust transportation to the east Asia region including Japan.

[19] From 2000 to 2001, dust events have been frequently observed in the cities of northeast China, Korea and Japan. On the basis of the meteorological data, it was found that in this period strong winds often blew which led to dust storms

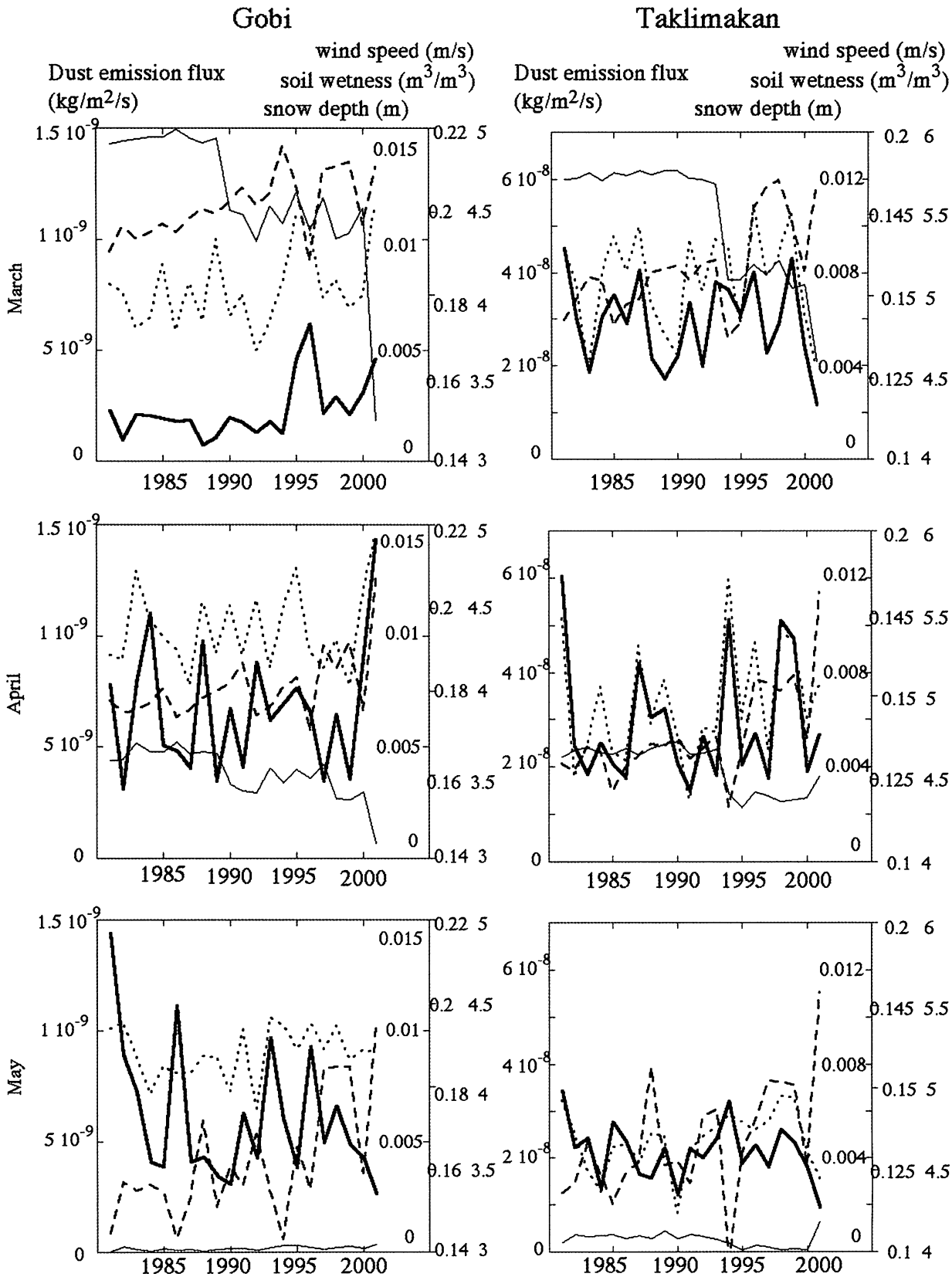

Figure 7. Monthly mean time series of the dust emission flux (thick solid lines, kg/m^2/s) in the Gobi and the Taklimakan deserts from March to April. Time series of controlling factors are also shown for wind speed near the surface (thin dashed lines, m/s), soil wetness (thick dashed lines, m^3/m^3), and snow depth (thin solid lines, m).

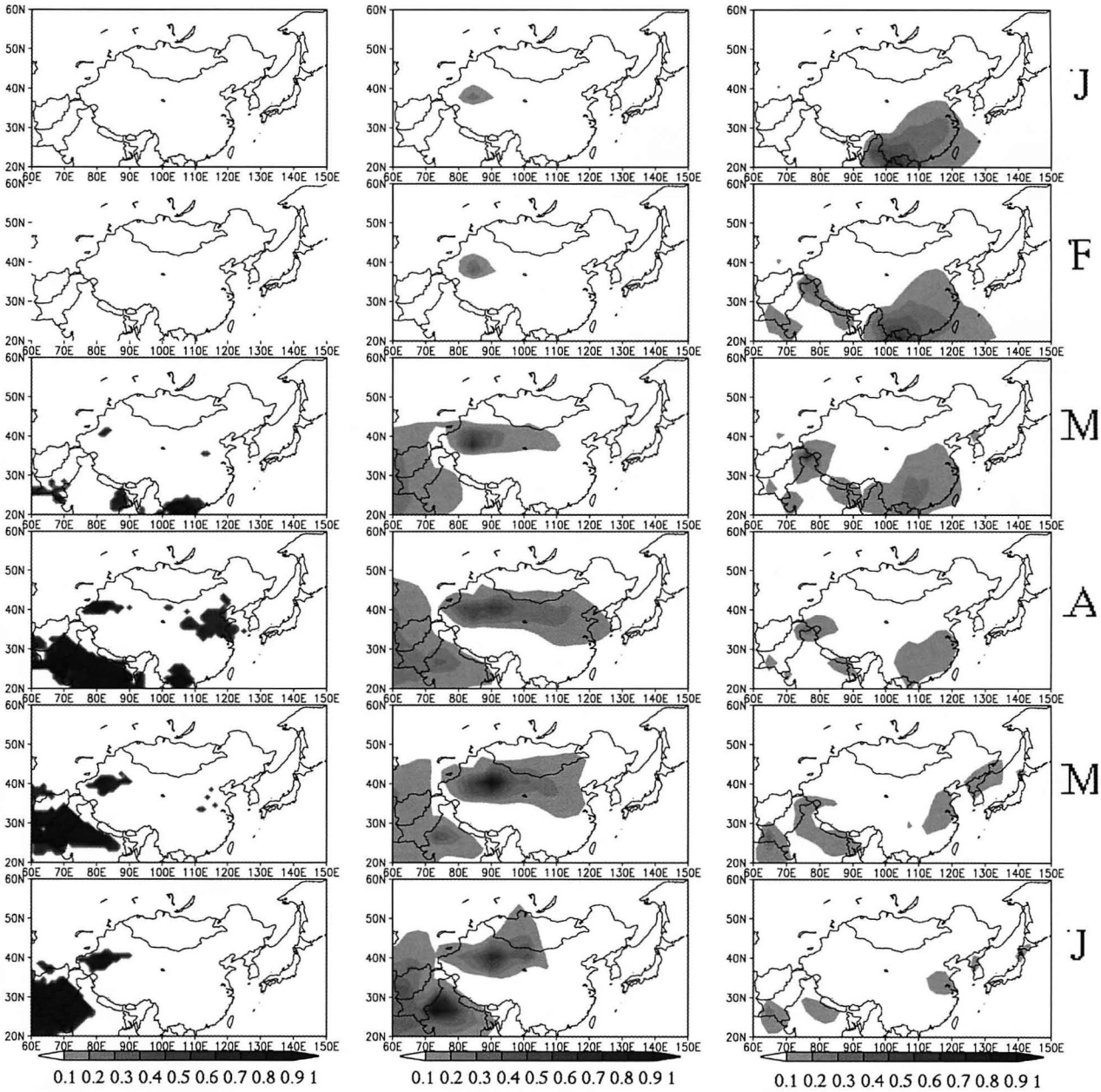

Figure 8. Monthly mean Total Ozone Mapping Spectrometer (TOMS) aerosol index (left columns), simulated dust aerosol optical thickness at 550 nm (middle columns), and simulated carbonaceous aerosol optical thickness at 550 nm (right columns) in 2000.

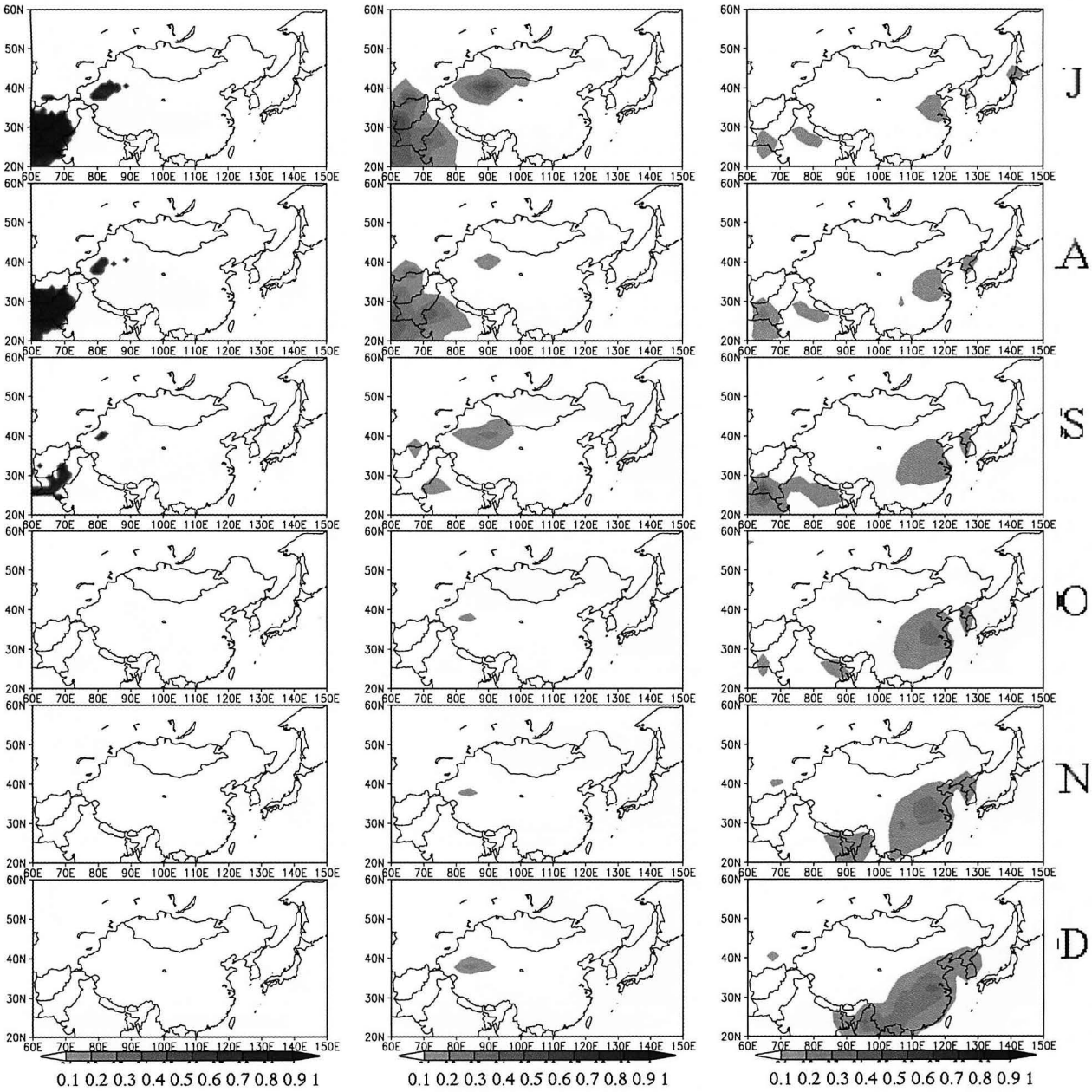

Figure 8. (continued)

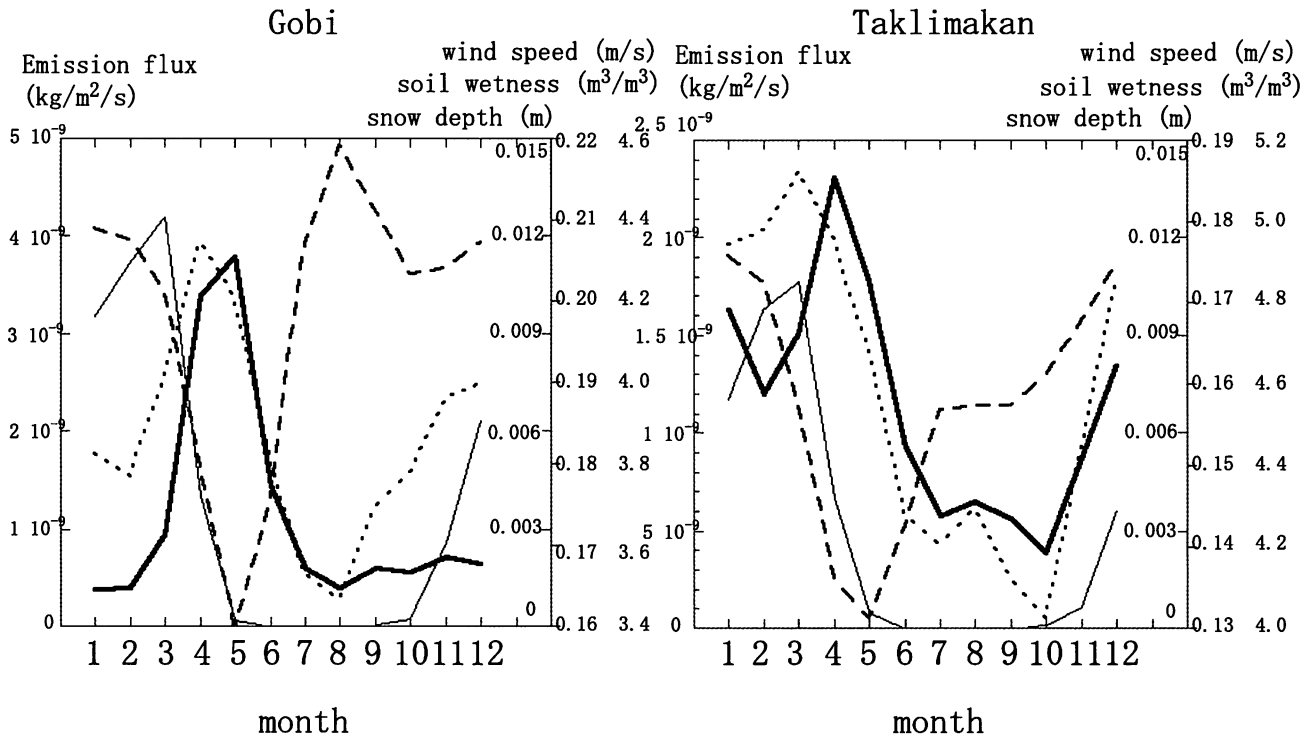

Figure 9. Monthly mean dust emission flux (thick solid lines, kg/m^2/s) in the Gobi and the Taklimakan deserts. Seasonal variation in the controlling factors is also shown for wind speed near the surface (thin dashed lines, m/s), soil wetness (thick dashed lines, m^3/m^3), and snow depth (thin solid lines, m).

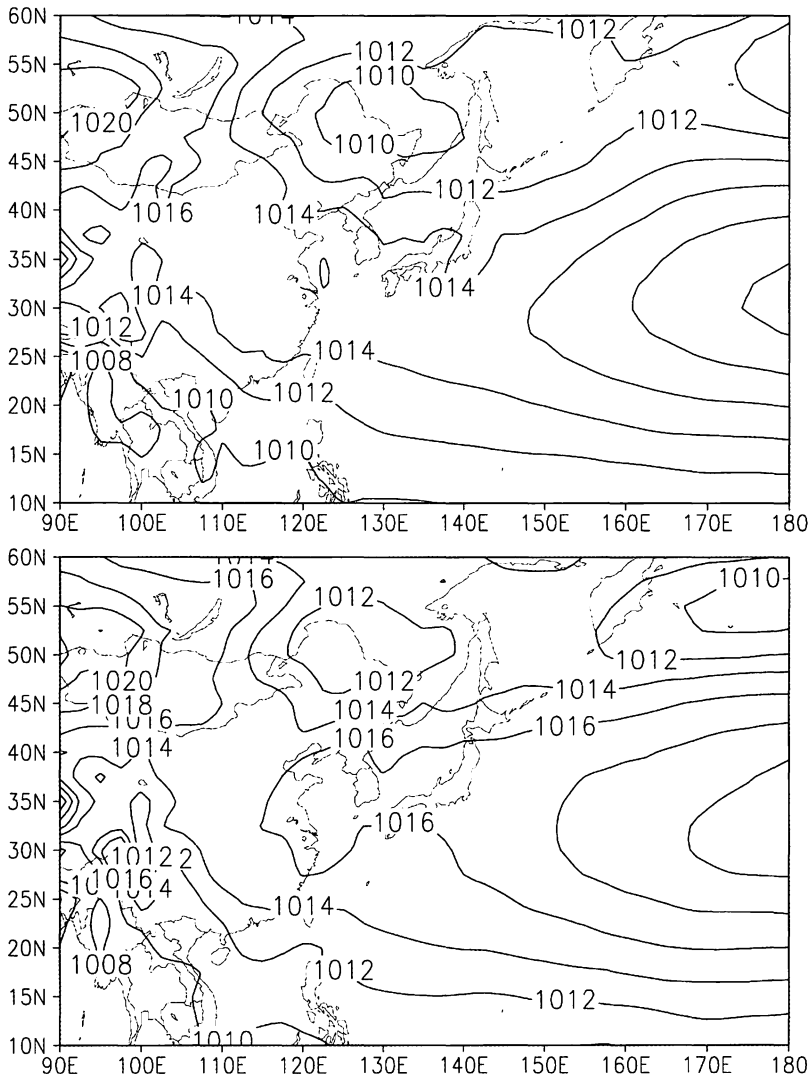

Figure 10. April mean sea level pressure (hPa) in high-frequency years and low-frequency years.

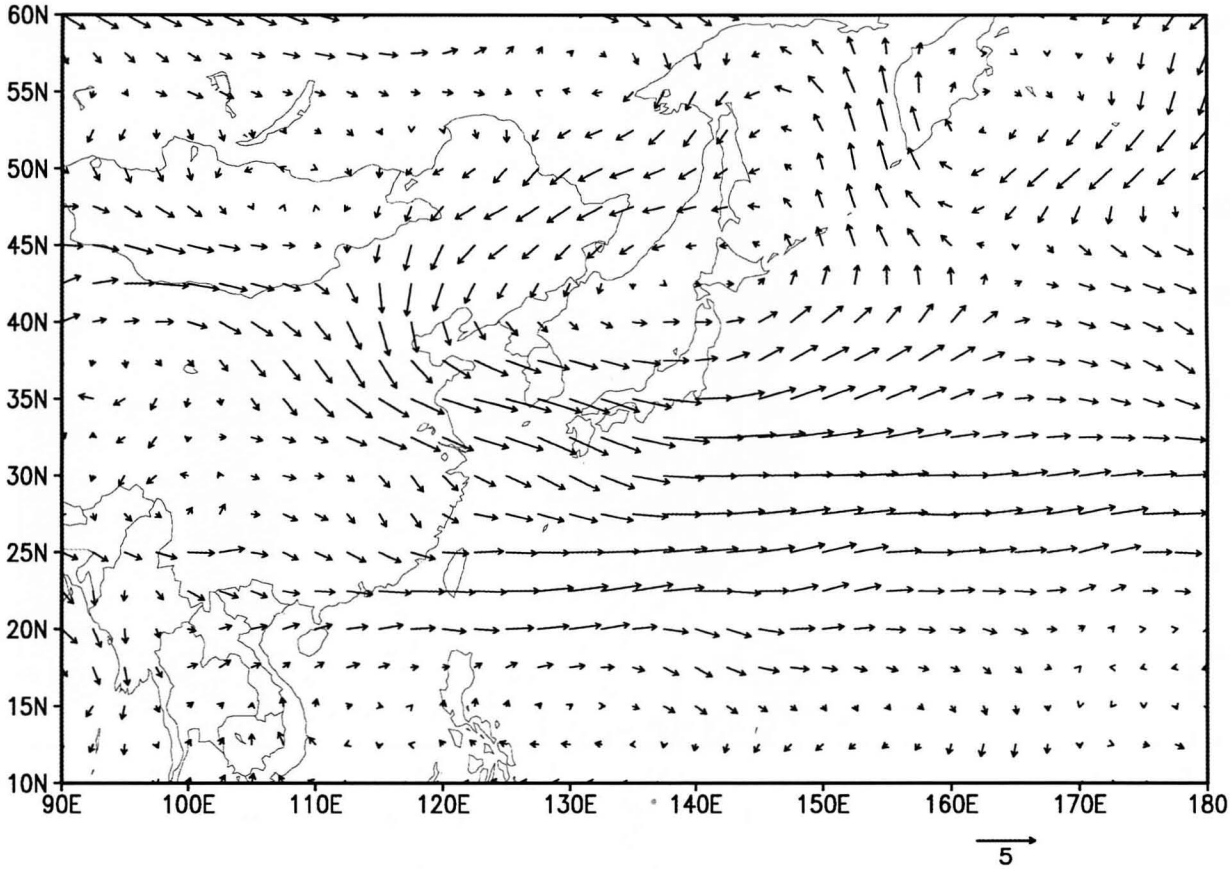

Figure 11. Difference in April mean 700 hPa wind speed (m/s) between high-frequency years and low-frequency years.

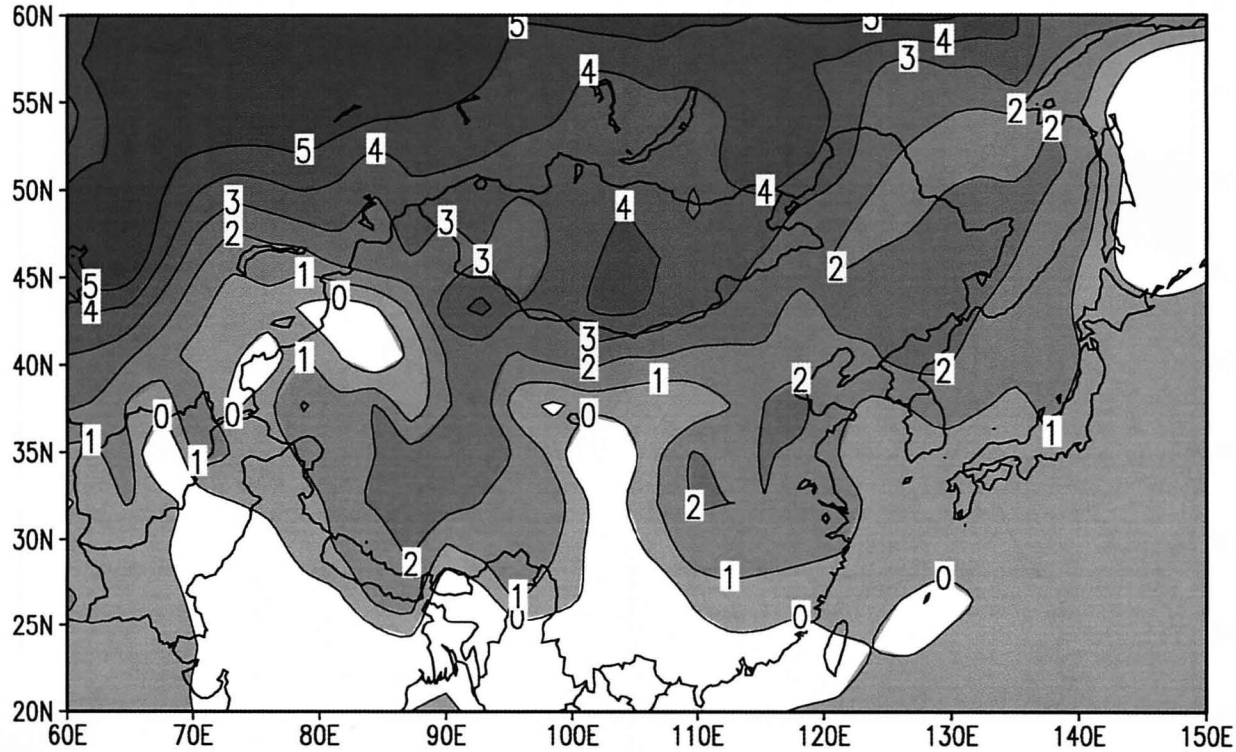

Figure 12. Difference in March mean surface temperature (K) between high-frequency years and low-frequency years.

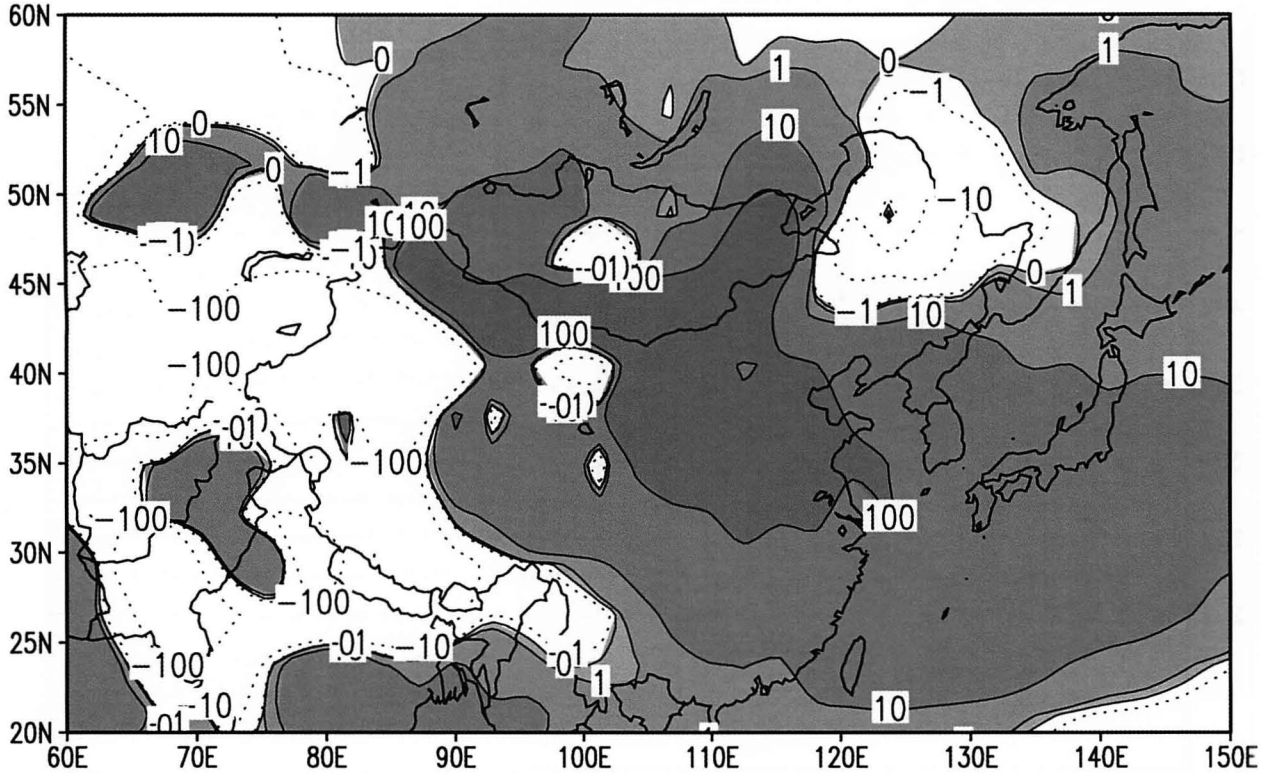

Figure 13. Difference in simulated April mean dust mass concentrations ($\mu g/m^3$) between high-frequency years and low-frequency years.

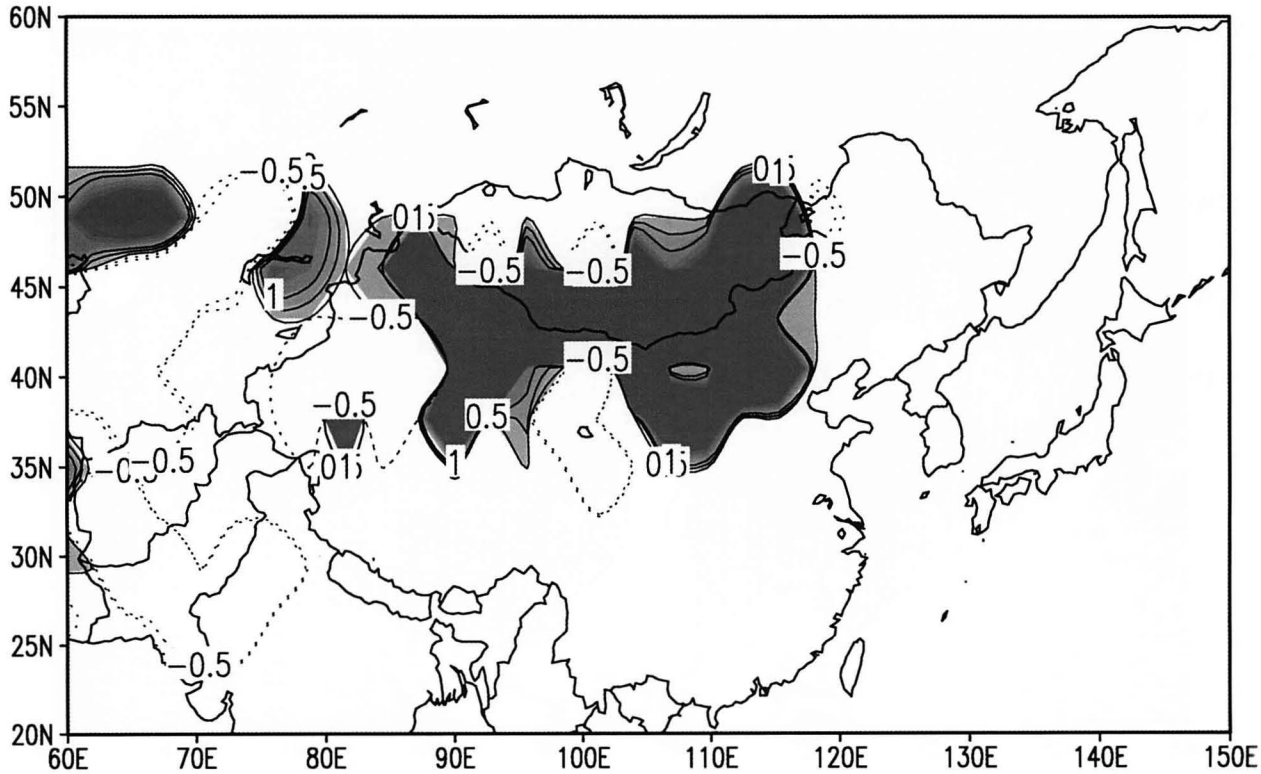

Figure 14. Difference in simulated April mean dust emission fluxes ($\mu g/m^2/s$) between high-frequency years and low-frequency years.

in the Gobi desert and northeast China. The model simulation also shows an increase in dust emission from the Gobi desert and northeast China from 2000 to 2001, despite decreasing dust emissions in the western part including the Taklimakan desert. However, the simulated aerosol mass concentration in Japan does not reproduce this sudden increase such as in the observed *Kosa*-days. One of the reasons for this discrepancy is that potential dust emission locations are fixed in this model. There are reports that desertification and land use changes in the northeastern China are significant, so that we may need to introduce such temporal changes in the land surface conditions in the model for better simulation of the time series. Location dependence of the large disagreement between the time series of simulated dust emission flux and observed dust storm day numbers as shown in Figure 4 also suggests that the problem in the surface modeling is serious. It is difficult at our present research stage, however, to conclude that such improvement in the surface model can produce a better decreasing trend in the 1990s. The quality of the objective analysis meteorological data will be another issue for better simulation of the long-term trend in dust events. We would like to improve our model for future simulations of the dust events after detailed investigations of the impact of easing the current problems as suggested in the present study.

[20] **Acknowledgment.** This work was supported by the Japan Science and Technology Agency/CREST/APEX project.

References

Chun, Y., K. O. Boo, J. Kim, S. U. Park, and M. Lee (2001), Synopsis, transport, and physical characteristics of Asian dust in Korea, *J. Geophys. Res.*, *106*, 18,451–18,469.

Gillette, D. (1978), A wind tunnel simulation of the erosion of soil: Effect of soil texture, sandblasting, wind speed and soil consolidation on dust production, *Atmos. Environ.*, *12*, 1735–1743.

Kalma, J. D. (1988), Potential wind erosion in Australia: A continent perspective, *J. Climatol.*, *8*, 411–428.

Kinne, S., et al. (2003), Monthly averages of aerosol properties: A global comparison among models, satellite data, and AERONET ground data, *J. Geophys. Res.*, *108*(D20), 4634, doi:10.1029/2001JD001253.

Matthews, E. (1983), Global vegetation and land use: New high-resolution data bases for climate studies, *J. Clim. Appl. Meteorol.*, *22*, 474–487.

Nakajima, T., et al. (2003), Significance of direct and indirect radiative forcings of aerosols in the East China Sea region, *J. Geophys. Res.*, *108*(D23), 8658, doi:10.1029/2002JD003261.

Numaguti, A., M. Takahasi, T. Nakajima, and A. Sumi (1995), Development of an atmospheric general circulation model, in *Climate System Dynamics and Modeling*, edited by T. Matuno, pp. 1–27, Cent. for Clim. Syst. Res. Univ. of Tokyo, Tokyo.

Qian, W., and Y. Zhu (2001), Climate change in China from 1880 to 1998 and its impact on the environmental condition, *Clim. Change*, *50*, 419–444.

Qian, W., L. Quan, and S. Shi (2002), Variations of the dust storm in China and its climatic control, *J. Clim.*, *15*, 11,216–11,228.

Sun, J., M. Zhang, and T. Liu (2000), Spatial and temporal characteristics of dust storms in China and its surrounding regions, 1960–1999: Relations to source area and climate, *J. Geophys. Res.*, *106*, 10,325–10,333.

Takemura, T., H. Okamoto, Y. Maruyama, A. Numaguti, A. Higurashi, and T. Nakajima (2000), Global three-dimensional simulation of aerosol optical thickness distribution of various origins, *J. Geophys. Res.*, *105*, 17,853–17,873.

Takemura, T., T. Nakajima, O. Dubovik, B. N. Holben, and S. Kinne (2002a), Single scattering albedo and radiative forcing of various aerosol species with a global three-dimensional model, *J. Clim.*, *15*, 333–352.

Takemura, T., I. Uno, T. Nakajima, A. Higurashi, and I. Sano (2002b), Modeling study of long-range transport of Asian dust and anthropogenic aerosols from East Asia, *Geophys. Res. Lett.*, *29*(24), 2158, doi:10.1029/2002GL016251.

Takemura, T., T. Nakajima, A. Higurashi, S. Ohta, and N. Sugimoto (2003), Aerosol distributions and radiative forcing over the Asian-Pacific region simulated by Spectral Radiation-Transport Model for Aerosol Species (SPRINTARS), *J. Geophys. Res.*, *108*(D23), 8659, doi:10.1029/2002JD003210.

Yang, G. (2002), Black wind storm in northwest China: A case study of the strong sand-dust storm on May 5th, 1993, in *Global Alarm: Dust and Sandstorms from the World's Drylands*, edited by Y. Yang, V. Squires, and Q. Lu, pp. 49–73, U.N. Conv. to Combat Desertification, New York.

Yoshino, M. (2001), Kosa (Asian dust) related to Asian monsoon system, paper presented at the 3rd International Symposium of Asian Monsoon System (ISAM3), Univ. of Tokyo, Okinawa, Japan.

M. Mukai and T. Nakajima, Center for Climate System Research, University of Tokyo, 4-6-1 Komaba, Meguro-ku, Tokyo 153-8904, Japan. (mukai@ccsr.u-tokyo.ac.jp; teruyuki@ccsr.u-tokyo.ac.jp)

T. Takemura, Research Institute for Applied Mechanics, Kyushu University, 6-1 Kasuga-koen, Kasuga, Fukuoka 816-8580, Japan. (toshi@riam.kyushu-u.ac.jp)